Nuclear Instruments and Methods in Physics Research A 00 (1994) NIM01304
North-Holland

NUCLEAR INSTRUMENTS & METHODS IN PHYSICS RESEARCH
Section A

Position-sensitive fiber readout

D.C. Fries, M. Kaiser, S. Rohr
Institut für Exp. Kernphysik, Universität Karlsruhe, Germany

Received 11 March 1994

The possibility has been investigated to separate the signals from scintillating fibers in a fiber detector array by optical delay, thus providing the possibility to read-out several fibers with a single photomultiplier. Measuring basic fiber properties of PS and PMMA fibers, in particular the propagation and dispersion of light pulses we found that a separation of up to ten adjacent fibers can be achieved by optical delay. Limits of this method have been discussed and ways to improve the present limits have been indicated.

1. Introduction

Scintillating fibers arranged parallel to each other in a planar array can be used as a counter plane for particle hodoscopes and as a detection plane in a total energy counter, such as an electromagnetic or hadron calorimeter.

Devices of this type have been used successfully in a number of high energy experiments [5,7,4]. Its advantage lies in the fact that it combines a high spatial resolution and a fast response time with a good detection efficiency. The design of an efficient read-out system for an array of the plastic fibers, which utilizes the high inherent spatial and time resolution requires a major technical (and financial) effort, if one uses means such as multichannel photomultipliers, or a CCD readout.

In this paper we present a study of the possibility to localize a fiber in a detector array by delaying its signal optically, using non-scintillating, "clear" plastic fibers as optical delay lines.

The paper is organized as follows: in section 1 we report on measurements of the relevant properties of scintillating and clear plastic fibers and of their couplings.

In section 2 we discuss measurements of the signal propagation and its time resolution in plastic fibers.

In section 3 we investigate the possibility to read out an array of several fibers with a single photomultiplier by using optical delaylines.

2. Relevant properties of plastic optical fibers

2.1. Experimental setup

For the experimental investigation of fiber properties such as the attenuation, the propagation and the time dispersion of a light pulse a measuring bench has been constructed consisting of a 6 m long U-shaped channel, covered by a lid, in which optical fibers to be measured can be subtended. The far end of the fiber is connected to the cathode of a photomultiplier (PM). A source for feeding a localized light signal into the fiber to be measured is mounted on a carriage, which can be moved along the fiber by a remote control.

Several methods have been applied to generate pulsed light signals for this purpose:

– In a *scintillating* fiber a light signal can be generated by illuminating the fiber at a chosen point with the output of a pulsed ultraviolet nitrogen laser [#1]. A light pulse in a clear fiber can be obtained by optically coupling the scintillating fiber to the clear one.

With this methods we obtained light pulses in the range of 420 nm [#2], which have a width of 3 ns and a repetition rate of about 20 Hz. The intensity of a Laser-generated signal in a scintillating fiber was equivalent to about several hundred photoelectrons in the PM.

A similar result has been achieved by converting the ultraviolet laser light in a blocklet of scintillating material, which is optically coupled to the fiber to be measured.

– Since the fiber techniques is to be applied for the detection of charged particles we have used also minimum ionising particles (MIPs) crossing a scintillating fiber as a source for light pulses. With electrons from a beta source (^{90}Sr) one obtains light signals, whose intensity corresponds to about 7 photoelectrons.

Fig. 1 shows the mobile carriage in the measuring channel from where the light pulses are coupled into the subtended fiber to be measured.

For the detection of the light signals served a ten-stage photomultiplier with a bialkhali cathode (Hamamatsu R-

[#1] Wavelength = 337 nm, power output = 20 μJ per pulse.
[#2] This value corresponds to the mean of the optical spectrum of the tested scintillating fibers.

SSDI 0168-9002(94)00504-Z

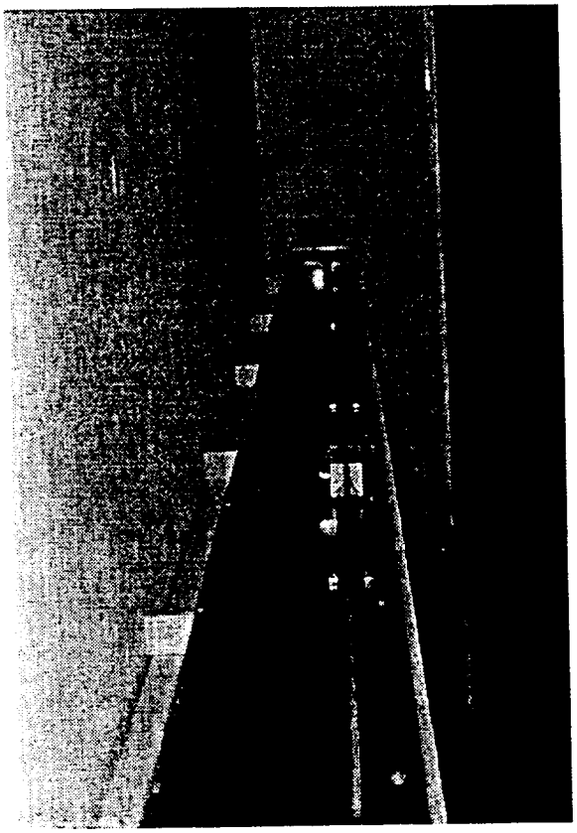

Fig. 1. The optical channel.

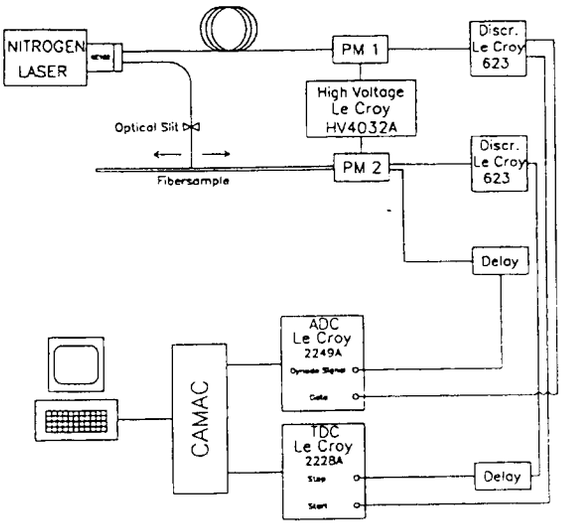

Fig. 2. Experimental setup.

647). The pulse height and the time structure of the PM output were analysed with a conventional ADC, a leading edge or constant-fraction discriminator together with a time-to-digital converter (TDC). A second photomultiplier receiving a lightsignal directly from the Laser served as a monitor of the Laser intensity and provided a gate and a start signal for the measurements of the light propagation. The data were read through CAMAC to a Lab-computer. The experimental setup is shown in Fig. 2.

2.2. *Properties of scintillating and clear fibers*

We investigated graded scintillating and clear fibers of a diameter of 1 mm. The scintillating fibers having a polystyrol (PS) base are doped with a scintillating agence such as terphenyl or polyphenyloxyd.

The clear fibers have a polyacryl base (PMMA; Polymethyl-methacrylate). The essential parameters of the optical fibers, such as the critical angle θ_c, being the angle of total reflection in the core of the fiber, the numerical aperture $A_N = n_c r \sin \theta_c = \sqrt{n_c r^2 - n_c l^2}$ (where $n_c r$ and $n_c l$ are the refractive indices of the core and the cladding area, respectively) are listed in Table 1.

For the transmission of optical signals through plastic fibers the losses are of primary interest. We measured therefore at first the attenuation length λ of both, the PMMA and the PS fibers.

The experimental procedure consisted of the determination of the ADC spectra of the transmitted light signal as a function of the distance between the location of the light input into the fiber and the detector. The graded fibers show a different attenuation length when measured near the location, where the signal is created or far away. This is due to the different transmission properties in the core and cladding region respectively. The decay lengths λ in both areas, in the core and the cladding region, can be measured separately by optically isolating one or the other [6]. In order to isolate the light transmission along the

Table 1
Properties of the scintillating and clear fibers

PS fibers							
Type	θ_c	θ_m	A_N	λ_{cr} [m]	λ_{cl} [m]	Δ_A [%]	Δ_T [%]
BCF12	21.3°	35.5°	0.58	4.60 ± 0.5	1.9 ± 0.3	21.0	29.0
S101A	27.3°	46.9°	0.73	2.20 ± 0.17	0.97 ± 0.07	34.0	41.0
PHT43	21.0°	34.8°	0.57	4.13 ± 0.5	1.87 ± 0.12	20.0	27.0
Clear fiber (PMMA)							
FEK40	18.4°	28.8°	0.47	14.5 ± 1.3	–	–	11.0

cladding area of the fiber, the fiber was glued into Lucite block using an Epoxyd glue ($n = 1.57$), in such a way, that the light from the cladding area is refracted away from the core.

By masking off either areas of the fiber, we obtained the attenuation length λ_{cr} of the core and λ_{cl} of the cladding area for the fiber types, which we have tested, see Table 1. One notices, that λ in the cladding area is – due to the unprotected outer surface of the fiber – substantially smaller than in the core.

2.3. Fiber-to-fiber connectors

Since the optical coupling of two fibers induces major signal losses, some care is needed in constructing an efficient connector. We have tested different methods of coupling.

Two fibers can be joined in a tide bore drilled through a small blocklet of about 3 cm length by either glueing or pressing the polished fiber end-faces together. (The material of the blocklet can be Lucite or even metal).

Another method yielding often satisfactory results consists of welding the two fibers together by applying heat to the joint [1]. A controlled heating procedure seems however mandatory. Two fibers can also be joined in a triangular groove, which is cut in to the flat surface of a plate of material, pressing a counterpiece against the plate, thus holding the fibers rigidly in its position, see Fig. 3. Connectors of these types have been manufactured and tested for single fibers; using an array of bores or grooves, the method is also applicable for a multitude of fibers.

The fiber connection causes essentially two types of losses in the transmission of the light signal:

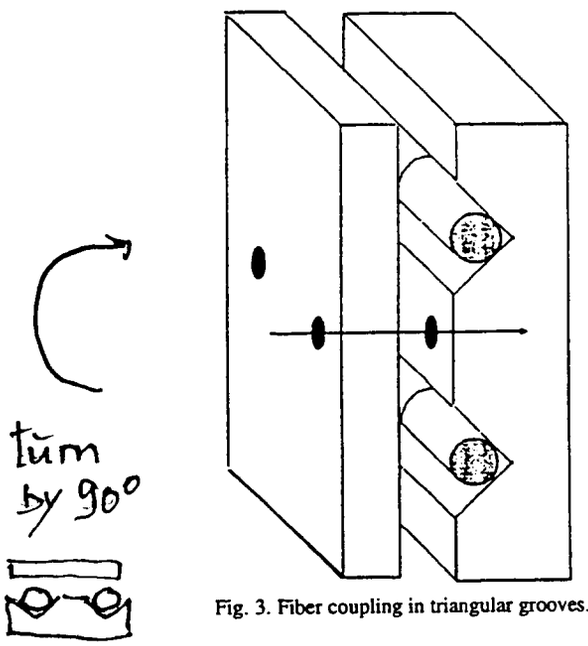

Fig. 3. Fiber coupling in triangular grooves.

Table 2
Transmission losses after each step of work

Work done	Rel. loss [%]
(a) cutting the fiber with pliers	49.6
(b) polishing with abrasive paper (120)	33.4
(c) polishing with abrasive paper (360)	15.9
(d) polishing with polishing paper	12.9
(e) polishing with polishing filt	12.1
(f) silicon grease	11.3

– The mismatch of the numerical apertures of the two fibers to be coupled.

– The mechanical misalignment and the optical quality of the fiber endfaces to be joined.

The loss due the aperture effect Δ_A and the total transmission loss Δ_T of the coupling of the scintillating to clear fibers have been determined for every fiber and are shown in Table 1.

Measuring the transmission loss of two clear fibers joined in a groove connector we determined the influence of the cutting and polishing procedure and the usage of silicon grease. The transmission losses after each (sequential) step of work are listed in Table 2.

In contrast to the PMMA fibers, PS fibers are quite sensitive to mechanical bending, which causes a permanent reduction of the effective attenuation length. We measured the bending effect and the resulting hysteresis effect as a function of time. A bend with a radius of 20 mm, about 25 cm downstream from the signal input introduces a short section of high absorption and reduces the effective attenuation length by about 60%. This can be seen comparing the bending effect on area upstream and downstream from the bending location, see Fig. 4. It was found that a circular bend of a PS fiber with a radius smaller than 20 mm yields a permanent reduction of the attenuation length λ. We have observed an asymptotic 10% recovery of λ over a period of several hours.

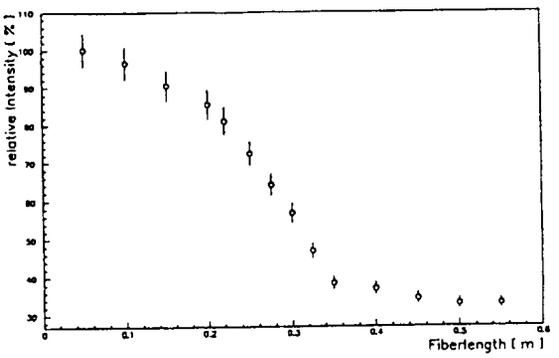

Fig. 4. Signal reduction due to mechanical bending of a PS fiber.

Table 3
Light yield in the scintillating fibers; $\tilde{\mu}$ corresponds to μ averaged over the fiber thickness

Type	$\tilde{\mu}$ [p.e./MIP]	χ^2/f ($f \approx 20$)
BCF12	7.4 ± 0.6	1.5
S101A	5.3 ± 0.5	1.4
PHT43	8.0 ± 0.6	1.8

2.4. Light yield

The light output of the scintillating fiber, is usually given in terms of the average number of photoelectrons produced by a MIP traversing the fiber. We evaluated the light efficiency using a ^{90}Sr beta source in a twofold coincidence, requiring, that the electrons cross the fiber perpendicular to the fiber axis at a distance $l = 5$ cm from the fiber end (PM).

Assuming that the photoelectrons due to the energy deposit of charged tracks in the scintillating fiber are Poisson-distributed and considering the geometrical shape of the fiber, the probability of observing n photoelectrons from a charged track crossing the scintillating fiber obtained by averaging over the fiber cross section can be written [6]:

$$P(n;\, \mu,\, r) = \int_0^r \frac{x/r}{\sqrt{r^2 - x^2}} \frac{e^{-2\mu x}(2\mu x)^n}{n!}\, dx.$$

Here μ is the mean number of produced photoelectrons per unit path length in the fiber, and r is the radius of the scintillating fiber. By fitting the Monte Carlo generated distribution $P(n;\, \mu,\, r)$ to the measured ADC-spectra, we determined the effective mean number $\tilde{\mu}$ of photoelectrons per MIP crossing the scintillating fiber, see Table 3. The average energy deposit in the fiber is about 0.23 MeV.

The effective loss due to attenuation of the signal in the PS fiber can be reduced by reading the signal from both ends of the fiber. In Fig. 5 the attenuation of the scintillation signal is shown as a function of length, reading the fibers from one and both sides. The exponential curve, fitted to the data points of the one side readout, shows the attenuation of the light signal in the fiber.

3. Signal propagation, time resolution and intermodal dispersion

We tested the possibility to identify a fiber in an array of scintillating fibers by feeding several fibers to the same photomultiplier (PM) and using different optical delays for each fiber. The signal arrival time thus associates each fiber with a fiber address.

Decisive problems of this technique are the time resolution and the attenuation of light pulses after propagation through optical delaylines.

Since the signal from a MIP crossing a single fiber produces about 7 photoelectrons, optical fibers, to be used as delaylines, cannot be made much longer than one or two attenuation lengths. The effective propagation time of a light pulse in a PMMA fiber, has been measured to be 5.08 ± 0.1 ns/m, allowing a total delay of 75–150 ns.

3.1. Time resolution and correction of the arrival time of optical pulses

In order to study the distribution and the resolution of the arrival time of a light pulse propagating in an optical fiber, a threshold (leading edge) discriminator was used to generate a stop pulse for a time-to-digital converter (TDC). The experimental set up was essentially identical with Fig. 2.

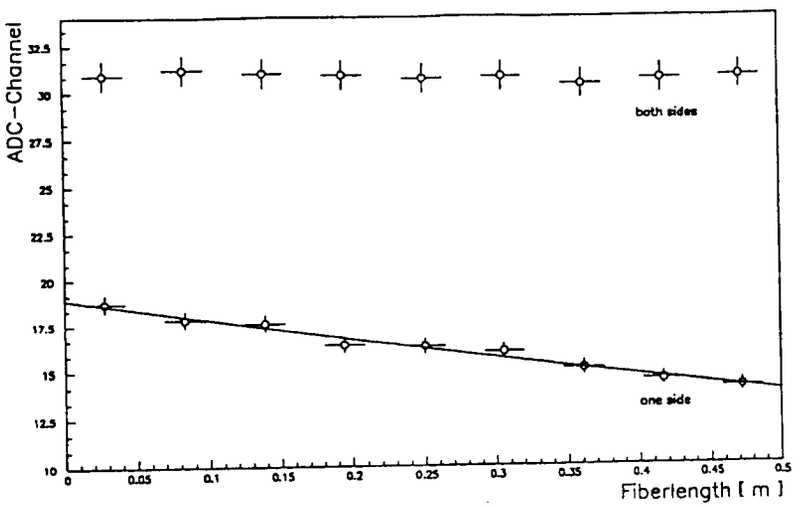

Fig. 5. Signal from the scintillating fiber, read from one side, and from both sides.

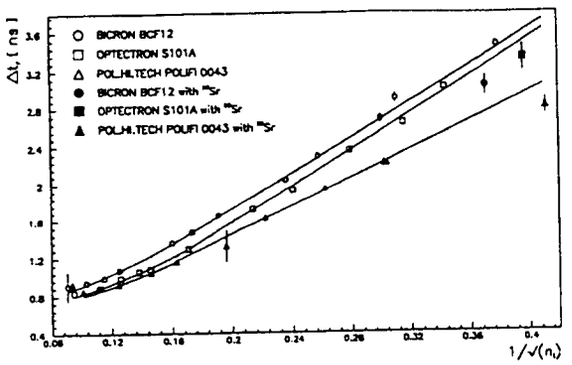

Fig. 6. Time resolution as function of number of photoelectrons.

Using an optical slit, the intensity of the Laser light coupled into the scintillating fiber, was varied yielding between 3 and 70 equivalent photoelectrons. The effective arrival time t_r of a light pulse is defined by the stop pulse for the TDC. The mean t_r being shifted by the pulse height dependence of the threshold discriminator and the distortion of the signal in the preceeding electronics (PM/cables) depends therefore on the number of effective photoelectrons [#3]. The measured arrival time t_r can be corrected for that electronic "walk", if its dependence on the pulse height is known. The time resolution, that is the fluctuation Δt_r of the pulse arrival time, defined as the FWHM of the measured time spectrum [2,3]. Δt_r was measured as a function of the number of photoelectrons n_i. As we used Laser signals as input, varying the intensity, n_i was computed from the charge collection at the ADC, which has been calibrated.

Fig. 6 shows Δt_r as a function of $1/\sqrt{n_i}$ for the three types of scintillating fibers. In addition we added in Fig. 6 low signal measurements using the beta source data. Fig. 6 indicates that for small signals the fluctuations are dominated by the Poisson statistics of the photoelectrons available. For large signals the time resolution Δt_r tends to become constant at a value of $\Delta t_r \approx 0.8$ ns. This may be due to the properties of the scintillating material in the fibers and to the pulse distorsion connected with the PM. The Laser and the beta source data, exhibiting the $1/\sqrt{n_i}$ dependence, are in reasonable agreement. The differences between the three fibers tested, indicate that a small value of the decay time τ of the scintillating material improves the time resolution. Table 4 shows for the three types of scintillating fibers, the photoelectron yield n_i and the time resolution Δt_r together with the typical decay time τ of the corresponding scintillator type.

For the determination of the correction on the arrival time t_r we measured t_r relative to a fixed start time t_0 as a function of pulse height, setting the threshold discriminator

[#3] Extensive tests with a 'constant-fraction'-discriminator have yielded no better results in the domain of very small signals.

Table 4
Measured time resolution with the beta source ^{90}Sr for different fiber types

Type	τ [ns]	n_i (^{90}Sr)	Δt_r (^{90}Sr) [ns]
BCF12	3.3	7.27 ± 0.12	3.05 ± 0.02
S101A	> 3.0	6.36 ± 0.1	3.33 ± 0.03
PHT43	1.0	5.9 ± 0.1	2.82 ± 0.02

to a minimal value. Fig. 7 shows $t_r(N)$ distributed as a function of the signal amplitude measured in terms of the number of ADC channels N.

The solid line represents a fitted function, whose general form

$$t_r(N) = a + \frac{b}{N} + c \log N$$

has been obtained from an theoretical analysis of the RC network of the electronics, where the photomultiplier was taken as a current source yielding a signal with a linear rise in time. (For signal amplitudes very close to the discriminator threshold the above fitting function did not describe the data and was replaced by a quadratic polynomial form.)

For the measurements of the time resolution Δt_r this pulse height dependent effect has been corrected by an offline analysis. In this way the values of time resolution could be improved up to 8%.

3.2. Dispersion of the arrival time of optical pulses

In addition to the effects mentioned before also the time dispersion of the propagating pulse influences the distribution of t_r. It is known that the intermodal dispersion has the effect to shift and to widen the single light pulse, reducing the amplitude and shifting the effective t_r to greater values [8]. Its origin is the fact that photons propagating through the fiber, can have a wide range of entrance angles, depending on the light source. Hence

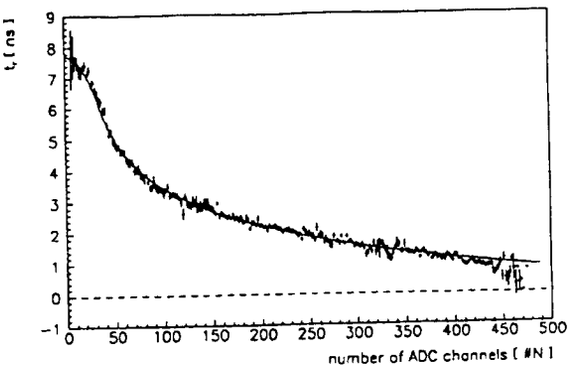

Fig. 7. t_r as function of signal amplitude measured with a leading edge discriminator.

different photons have different paths length and different propagation time in the fiber related to their angle of entrance, leading to an average shift t_m of the effective arrival time.

A simulation of this effect for the PMMA fiber using Monte Carlo methods assuming a uniform distribution of the input angle and a Gaussian time distribution of the initial light signal, yielded for t_m a relative small value.

$$t_m = 0.17 \pm 0.01. \quad [ns/m]$$

Experimentally the effect of the intermodal dispersion has been confirmed approximately as an additional increase of t_r after correcting our measured data for the amplitude depending effects discussed before.

Hence, the intermodal dispersion causes only a slight lengthdependent delay for each fiber in the fiber array.

3.3. PM-induced delays for optical pulses

It has been found that the measured arrival time of the light pulses is strongly correlated with the location on the cathode surface, where the fiber interfaces the photomultiplier.

Different locations on the photocathode are associated with trajectories of different path length of the ensuing photoelectrons in the PM, hence with different transit times.

The position dependence was measured by interfacing laser-produced pulses, which are transmitted through a PMMA fiber to various positions on the photocathode of our PM, which has flat cathode surface of 1 cm sensitive diameter. The TDC was used to measure the effective arrival time. We scanned the photocathode surface systematically choosing 6 radial positions, starting from the center in steps of 1 mm, and scanning each radius azimutally in steps of 5°. The polar coordinate system was defined by the geometric center of the PM and an axis in direction of the pin no. 1 of the socket of the R647. The results are shown in Fig. 8 presented in a three-dimensional plot. It can be seen, that the effective delay of the recorded signals can reach several nanoseconds depending on the fiber location on photocathode. If one uses several fibers on the same cathode this effect has to be calibrated and will be an important correction for time measurements. One could envisage a multifiber read out system utilizing this effect to distinguish fibers by choosing a particular suited PM.

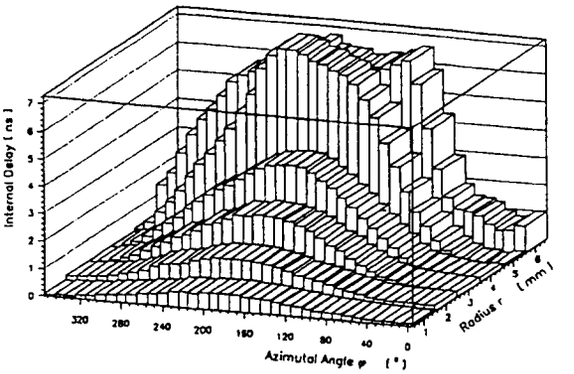

Fig. 8. Transmission time of the photoelectrons as function of the position on photocathode.

4. Fiber identification by optically delayed read-out

In order to test the possibility to distinguish by optical delays different fibers interfaced to the same photocathode by optical delay, we designed a metal frame subtending parallel ten scintillating fibers of 40 cm length. The fibers were connected on both ends to PMMA fibers which served as optical delaylines. The optical delay has been made different for each scintillating fiber by giving the

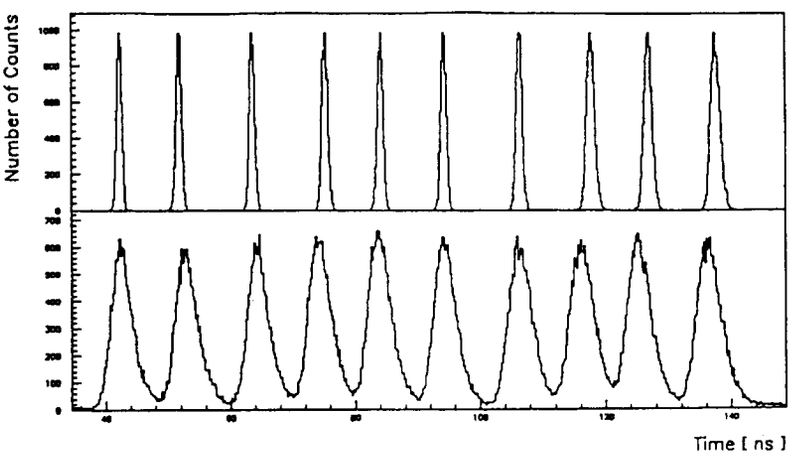

Fig. 9. Time distribution of 10 fibers measured with laser and beta source.

PMMA fibers different lengths. The differences were chosen 2, 4, 6, ··· 20 m, so the optical delays differed by about 10 ns. The 20 PMMA fibers were connected to the cathode surface of our PM.

As a first test we radiated Laser pulses through a pinhole collimater on to the scintillating fibers at a central position selecting the fibers one after another. The result is shown in the upper part of Fig. 9.

Since the light pulses corresponded each to about 100 photoelectrons the observed time dispersion was relatively small and therefore the separation of the fibers very good.

The slight broadening of time distributions, seen for the fibers with the longer delays indicates the reduction of the signal due to attenuation in the PMMA fiber.

Replacing the laser input by electrons from a ^{90}Sr source we placed a scintillation counter under the fiber to provide a stop pulse when an electron crossing a scintillating fiber delivered a start pulse for TDC.

Irradiating groups of the fibers with the beta source and collecting about equal numbers of signals for each fiber we obtained the distribution shown in the lower part of Fig. 9. Again we observe a clear separation of the ten fibers in their distribution of arrival time. The width of the distributions are considerably broader due to the correlation between time resolution and photon statistics, which was to be anticipated from our previous measurements.

The small unstructured background seen in Fig. 9 occurred essentially due to the fact that the geometrical matching of the fiber area and the stop counter was not perfect, and that we used no true coincidence.

No effort has been made to correct the time distributions for amplitude-depending effects. Systematic difference of the time delay between adjacent fibers, seen clearly for the laser data, reflect the fact, that the arrival time is shifted due to an internal delay in the PM, depending where the fiber is latched to the photocathode. This has been discussed in section 3.4. The probability to separate adjacent fibers by delay on the basis of this test, can be estimated to be about 96 percent.

Since the intensity of light pulses from electrons corresponded to about 2×6 photoelectrons (double sided readout), the total length of the optical delay lines cannot be made to much longer using comparable material. This problem can be overcome by using scintillating fibers however in several layers or with a larger cross section (2 mm). By increasing the effective number of photoelectrons one can increase the total delay and in addition reduce the delay differences between adjacent fibers.

The problem of double and multiple hits on a fiber has to be resolved – as for the comparable situation in wire chambers – by providing additional plaines with crossed fiber directions.

5. Conclusions

The possibility to separate the signals from scintillating fibers in a fiber detector array by optical delay has been investigated. Studying basic properties of PS and PMMA fibers, in particular the propagation and dispersion of light pulses, we found that a separation by optical delay up to ten fibers can be achieved with conventional means. An optical delay line of about 2.0 m PMMA fiber is sufficient to separate the adjacent fibers. The observed deterioration of the time resolution is due to the Poisson statistics of the low signal output per MIP of the scintillating fiber, in conjunction with the attenuation of the signal in the (delaying) PMMA fiber. As the laser measurements show the delayline could be considerably shorter if the signals were increased.

Our study indicates that with the method reported a lowcost scintillator array can be build with high spatial resolution, which can be used as a hodoscope or a measuring plane in a calorimeter. Improvements are possible in several ways:

a) by increasing the light output from the scintillating fiber choosing thicker scintillating fibers or foreseeing multilayered fiber array,

b) by finding fiber material with lower attenuation,

c) by utilizing the internal delay of the photomultipliers associated with the fiber position on the cathode.

Acknowledgement

We like to thank Dr. S. Weseler for discussion and a critical reading of the manuscript.

References

[1] G. Apollinari, Nucl. Instr. and Meth. A 311 (1992) 520.
[2] B. Bengston, Nucl. Instr. and Meth. 87 (1970) 109.
[3] B. Bengston, Nucl. Instr. and Meth. A 292 (1990) 329.
[4] D. Bernhard, Nucl. Instr. and Meth. A 315 (1992) 43.
[5] F.G. Hartjes, Nucl. Instr. and Meth. A 277 (1989) 379.
[6] C.M. Hawkes et al., Nucl. Instr. and Meth. A 292 (1990) 329.
[7] M. Kuhlen et al., Nucl. Instr. and Meth. A 301 (1991) 223.
[8] A.W. Snyder, J. Love, Optival Waveguide Theory (●● publisher, year).